HHS Public Access

Author manuscript

J Am Chem Soc. Author manuscript; available in PMC 2020 April 10.

Published in final edited form as:

J Am Chem Soc. 2019 April 10; 141(14): 5593–5596. doi:10.1021/jacs.8b12342.

^{68}Ga-NODAGA-indole, an allysine-reactive positron emission tomography probe for molecular imaging of pulmonary fibrogenesis

Jessica Wahsner[1], **Pauline Désogère**[1], **Eric Abston**[2], **Katherine A. Graham-O'Regan**[1], **Junfeng Wang**[1], **Nicholas J. Rotile**[1], **Markus D. Schirmer**[3], **Diêgo Dos Santos Ferreira**[1], **Jingyi Sui**[1], **Bryan C. Fuchs**[4], **Michael Lanuti**[2], and **Peter Caravan**[1]

[1]The Athinoula A. Martinos Center for Biomedical Imaging, The Institute for Innovation in Imaging, Department of Radiology, Massachusetts General Hospital (MGH) & Harvard Medical School (HMS), Charlestown, MA 02129, USA.

[2]Division of Thoracic Surgery, MGH & HMS, Boston, MA 02114, USA.

[3]Stroke Division, MGH & HMS, Boston, MA 02114, USA.

[4]Division of Surgical Oncology, MGH & HMS, Boston, MA 02114, USA.

Abstract

Oxidized collagen, wherein lysine residues are converted to the aldehyde allysine, is a universal feature of fibrogenesis, i.e. actively progressive fibrosis. Here we report the small molecule, allysine-binding positron emission tomography (PET) probe, ^{68}Ga-NODAGA-indole, that can noninvasively detect and quantify pulmonary fibrogenesis. We demonstrate that the uptake of ^{68}Ga-NODAGA-indole in actively fibrotic lungs is 7-fold higher than in control groups and that uptake is linearly correlated (R^2 = 0.98) with the concentration of lung allysine.

Graphical Abstract

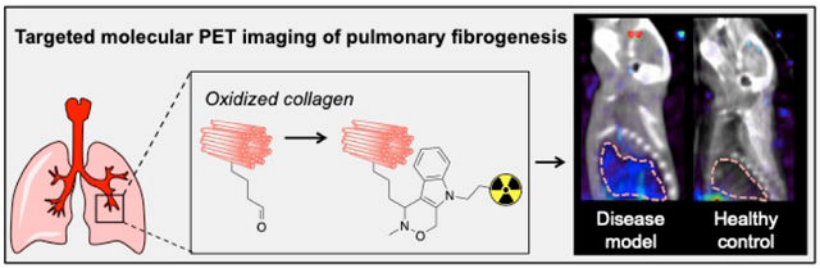

Pulmonary fibrosis is a respiratory disease that is a consequence of chronic tissue injury and is characterized by the accumulation of extracellular matrix (ECM) molecules that make up

Corresponding Author caravan@nmr.mgh.harvard.edu.

Supporting Information. Experimental details, synthetic procedures, compound characterization, structures of molecules not depicted in main text, additional HPLC traces, additional ex vivo analysis, additional fused PET/CT images, and PET data analysis. The Supporting Information is available free of charge on the ACS Publications website. (PDF)

The authors declare no competing financial interests.

scar tissue.[1] The progressive replacement of normal lung parenchyma with fibrotic tissue leads to impaired lung function and eventually death. Idiopathic pulmonary fibrosis (IPF) is the most common and the most lethal fibrotic lung disease with an estimated prevalence of 20 cases per 100,000 and a median survival of 3–5 years from the time of diagnosis.[2] IPF is a heterogeneous disease and there are no good tools to predict disease progression or to identify which patients may respond well to treatment. The ability to image disease activity (fibrogenesis) would allow clinicians to 1) identify which patients are likely to progress rapidly, 2) identify if a drug treatment is effective in reducing fibrogenesis, and 3) better stratify patients when evaluating new treatments in clinical trials.

There have been considerable efforts to develop non-invasive imaging agents able to detect and stage fibrotic disease to facilitate early diagnosis, to monitor disease progression and therapeutic response, and to advance drug development.[3–5] In the lung, high-resolution computed tomography (CT) can show extent of disease.[6] Direct targeting of collagen deposition that occurs during scar tissue formation with magnetic resonance imaging (MRI),[7] single photon emission computed tomography (SPECT),[8–9] or positron emission tomography (PET)[10–11] imaging probes has been used to image pulmonary fibrosis, but these probes measure total fibrosis and cannot distinguish actively progressive fibrosis from stable scar tissue.

A universal feature of fibrogenesis is the oxidation of collagen by the lysyl oxidase family of enzymes, which convert ECM lysine residues to the aldehyde allysine.[12] Allysine can undergo condensation reactions to crosslink collagen proteins, which in turn stabilizes the fibrotic ECM.[13] Recently, it was shown that pulmonary fibrogenesis can be imaged by targeting allysine with MRI probes.[14–15] Waghorn et al. employed an oxyamine functionalized derivative of Gd-DOTA capable of undergoing reversible condensation reactions with aldehydes to target allysine.[15] They observed 2-fold higher lung uptake of their targeted probe in an animal model of pulmonary fibrosis compared to naïve animals. We sought to develop a targeted PET probe to image fibrogenesis. PET is a quantitative imaging modality, and the very low mass dose used in PET results in an abbreviated preclinical development path to initiate human studies compared to MRI probes.

Here, we report the small molecule, allysine-targeted PET probe, ^{68}Ga-NODAGA-indole, and demonstrate its ability to detect pulmonary fibrogenesis by targeting oxidized collagen. It consists of the positron emitting ^{68}Ga isotope chelated by the 1,4,7-triazacyclononane-1-glutarate-4,7-acetate (NODAGA) chelator, a hydrophilic polyethylene glycol (PEG) linker, and an aminooxy-functionalized indole that rapidly forms hydrolytically stable condensation products with aldehydes at physiological pH (Fig 1a).[16]

We chose the NODAGA chelator for its ability to rapidly chelate ^{68}Ga and form stable complexes. The PEG linker increases hydrophilicity and reduces nonspecific protein binding. The aminooxy-functionalized indole was selected for its ability to form a hydrolytically stable C-C bond upon reaction with aldehydes (the Pictet-Spengler ligation). Unlike MRI contrast agents, that are administered in high concentrations (0.1 – 0.3 mmol kg^{-1}) and must be completely eliminated from the body after imaging, PET imaging requires extremely low mass doses (nmol, microgram mass range).[17] Consequently, *in vivo* labeling

with a targeted PET probe does not necessarily require a reversible reaction. We reasoned that formation of a hydrolysis resistant, covalent bond between Ga-NODAGA-indole and the allysine target would result in greater uptake in actively progressive pulmonary fibrosis. Moreover the aminooxy-functionalized indole features significantly enhanced condensation reaction kinetics at physiological pH compared to other oxyamine-based functionalities.[18–19] ^{nat}Ga-NODAGA-indole was prepared via condensation reaction between 2-(trimethylsilyl) ethoxycarbonyl (Teoc) protected indole **3** and chelator NODAGA-PEG-NH_2 (**5**), followed by complex formation using $^{nat}Ga(NO_3)_3$ in acetate-acetic acid medium at pH 4.5. Cleavage of the Teoc protection group with caesium fluoride yielded the final product ^{nat}Ga-NODAGA-indol (Supporting information, Scheme 1). As a negative control, we employed Ga-NODAGA-carboline, which is incapable of undergoing condensation reactions with aldehydes (Fig 1b). ^{nat}Ga-NODAGA-carboline was isolated after condensation reaction between indole **8** and chelator NODAGA-PEG-NH_2 (**5**), followed by complex formation using $^{nat}Ga(NO_3)_3$ in acetate-acetic acid medium at pH 4.5 (Supporting information, Scheme 2).

To validate the reactivity of Ga-NODAGA-indole towards aldehydes at pH 7.4, we treated 100 μM ^{nat}Ga-NODAGA-indole with 1.0 mM butyraldehyde in phosphate buffered saline (PBS) under pseudo first order conditions and monitored product formation by HPLC with an ICP-MS detector. The formation of the desired condensation product proceeded cleanly at room temperature (Fig. S1), with a second order rate constant of 0.29 ± 0.02 M^{-1} s^{-1}, which is similar to previously reported values for the aminooxy-functionalized indole moiety (Fig. S2).[16] We then investigated the binding of ^{nat}Ga-NODAGA-indole to tissue. The aorta is rich in allysine (μmol/g) due to high lysyl oxidase activity and high turnover of elastin and collagen.[20] Segments of porcine aorta (~ 25 mg) were incubated with either 200 μM of ^{nat}Ga-NODAGA-indole or ^{nat}Ga-NODAGA-carboline at 37 ˚C and pH 7.4 for 20 h. The aorta bound Ga was analyzed by ICP-MS. Figure 1c shows that ^{nat}Ga-NODAGA-indole binds to aorta tissue, whereas ^{nat}Ga-NODAGA-carboline showed negligible amounts of nonspecific binding. To demonstrate the specificity of the probe for tissue allysine, we pretreated segments of aorta with 4.0 mM 3-(2-(((methylamino)oxy)methyl)-1*H*-indol-1-yl) propanoic acid (**7**) (Supporting Information, Scheme 3), which exhibits the same aldehyde-reactive aminooxy functionality as Ga-NODAGA-indole. After blocking the aldehyde moieties in this manner, we incubated the pretreated aorta segments with each of the probes under the same conditions. We found similar negligible amounts of non-specific aorta binding for both probes, that were identical to the amounts of Ga-NODAGA-carboline taken up by untreated aorta tissue (Fig 1c).

Together, these observations confirm the ability of Ga-NODAGA-indole to specifically target aldehydes.

Both probes are very stable in human blood plasma over the course of 24 h at 37 ˚C, with respect to transmetallation or the formation of small molecule degradation species, as evaluated by HPLC-ICP-MS (Fig. S3 and S4).

Radiolabeling of the indole probe with ^{68}Ga was performed by applying a protecting group strategy to avoid any side reactions of the highly reactive aminooxy-functionalized indole, as

depicted in scheme 1. Fluorenylmethyloxycarbonyl (Fmoc) protected NODAGA-indole (**1**) was obtained via condensation reaction between Fmoc protected indole **11** and chelator NODAGA-PEG-NH_2 (**5**) (Supporting Information, Scheme 3). **1** was quantitatively radiolabeled in 5 minutes at 60 °C (Fig S5). Cleavage of the Fmoc protection group under basic conditions gave ^{68}Ga-NODAGA-indole without the need for HPLC purification (Fig S6). Radiolabeling of NODAGA-carboline (**10**) (Supporting information, scheme 2) to obtain ^{68}Ga-NODAGA-carboline was performed directly in 5 minutes at 60 °C and gave high radiochemical yields (> 99 %) (Fig S7).

We then evaluated the ability of ^{68}Ga-NODAGA-indole to detect fibrogenesis in a bleomycin mouse model of pulmonary fibrosis. Transtracheal instillation of bleomycin is a well-established method to cause pulmonary fibrosis in animal models.[21] We studied two groups of mice: i) mice injured with a single transtracheal instillation of bleomycin (BM, 1.0 unit/kg) and ii) mice that underwent a sham procedure with instillation of PBS only as a control group (SH). 13 – 15 days after instillation, the animals were injected intravenously with approximately 100 μCi of either ^{68}Ga-NODAGA-indole or ^{68}Ga-NODAGA-carboline. All animals were sacrificed for ex vivo analysis 2 h after administration of the different probes.

Bleomycin injury induced pulmonary fibrosis as demonstrated by Sirius Red histological staining where the presence of fibrosis is evident from the increase in areas stained in red (Fig S8). Hydroxyproline is a quantitative biomarker of collagen and hence, fibrosis.[22] We found that bleomycin-injured mice had a 1.5-fold higher hydroxyproline content in their lung tissue compared to sham animals (Fig S9). Allysine is a quantitative biomarker of fibrogenesis and bleomycin-injured mice exhibited a 2.0-fold higher allysine content in their lung tissue than sham animals (Fig S10).

The pharmacokinetics and biodistributions of ^{68}Ga-NODAGA-indole and ^{68}Ga-NODAGA-carboline were similar to each other in both sham and bleomycin injured mice (Fig 2a, S12-S16), with the exception of the lungs and liver. Both probes underwent rapid elimination from the blood (estimated $t_{½}$ = 6 – 9 min) through the kidneys into the urinary bladder and partly through the liver and gall bladder into the intestines. ^{68}Ga-NODAGA-indole showed higher liver uptake than ^{68}Ga-NODAGA-carboline (Fig 2a).

Bleomycin injury results in tissue edema and the wet lung weights of bleomycin injured mice are 2–3 times higher than that of uninjured mice. Therefore we compared lung uptake using the amount of probe per whole lung, Fig 2b. There was no significant difference between the lung uptake of ^{68}Ga-NODAGA-carboline in bleomycin- or sham-treated animals. On the other hand, the lung uptake of ^{68}Ga-NODAGA-indole in fibrotic lungs was 7-fold higher than in sham animals and 7 to 8-fold higher than the lung uptake of ^{68}Ga-NODAGA-carboline. The uptake of ^{68}Ga-NODAGA-indole in lung tissue correlates strongly (R^2 = 0.98) with allysine (Fig 2c), but less so with hydroxyproline (Fig S11, R^2 = 0.68) indicating that this probe may be a quantitative reporter of lung fibrogenesis and disease activity,

Fig 3 shows representative fused PET/CT sagittal images of the head and thorax 110 – 120 min post injection of either ^{68}Ga-NODAGA-carboline or ^{68}Ga-NODAGA-indole in bleomycin-injured or sham mice. ^{68}Ga-NODAGA-indole accumulates specifically in fibrotic lungs but not in the healthy lungs of sham animals, whereas ^{68}Ga-NODAGA-carboline showed no preferential uptake in fibrotic or healthy lungs.

In summary, we described the first small molecule PET probe that is able to detect and stage pulmonary fibrogenesis. ^{68}Ga-NODAGA-indole specifically binds to allysine in fibrotic lungs resulting in a 7-fold higher lung uptake in a disease model of pulmonary fibrosis in comparison to control groups. The uptake of ^{68}Ga-NODAGA-indole in lung tissue correlates strongly with the extent of actively progressive pulmonary fibrosis and provides a quantitative noninvasive measure of active disease. This molecular imaging ability of ^{68}Ga-NODAGA-indole makes it a promising candidate for monitoring disease progression and therapeutic response, and ultimately advancing drug development.

Supplementary Material

Refer to Web version on PubMed Central for supplementary material.

ACKNOWLEDGMENT

We thank the German Research Foundation (DFG, research fellowship 320225462, J.W.) and the NIH NHLBI (HL131907, P.C.) and OD (OD010650) for financial support. We thank Alana Ross, Dr. Derek J. Erstad, and Ian Ramsay for their help with the ex vivo biodistribution, Dr. Gengyang Yuan for his help with the PET images and Dr. Eman Aburieda Akam for many helpful discussions.

REFERENCES

(1). Friedman SL; Sheppard D; Duffield JS; Violette S, Therapy for Fibrotic Diseases: Nearing the Starting Line. Sci. Trans. Med 2013, 5 (167), 167sr1.

(2). Ahluwalia N; Shea BS; Tager AM, New Therapeutic Targets in Idiopathic Pulmonary Fibrosis. Aiming to Rein in Runaway Wound-Healing Responses. Amer. J. Resp. Crit. Care Med 2014, 190 (8), 867–878. [PubMed: 25090037]

(3). Baues M; Dasgupta A; Ehling J; Prakash J; Boor P; Tacke F; Kiessling F; Lammers T, Fibrosis imaging: Current concepts and future directions. Adv. Drug Delivery Rev 2017, 121, 9–26.

(4). Désogère P; Montesi SB; Caravan P, Molecular Probes for Imaging Fibrosis and Fibrogenesis. Chem. Eur. J 2019, 25 (5), 1128–1141. [PubMed: 30014529]

(5). Montesi SB; Désogère P; Fuchs BC; Caravan P, Molecular imaging of fibrosis: recent advances and future directions. J. Clin. Invest 2019, 129 (1), 24–33. [PubMed: 30601139]

(6). Noble PW; Barkauskas CE; Jiang D, Pulmonary fibrosis: patterns and perpetrators. J. Clin. Invest 2012, 122 (8), 2756–2762. [PubMed: 22850886]

(7). Caravan P; Yang Y; Zachariah R; Schmitt A; Mino-Kenudson M; Chen HH; Sosnovik DE; Dai G; Fuchs BC; Lanuti M, Molecular Magnetic Resonance Imaging of Pulmonary Fibrosis in Mice. Amer. J. Resp. Cell Molec. Biol 2013, 49 (6), 1120–1126.

(8). Muzard J; Sarda-Mantel L; Loyau S; Meulemans A; Louedec L; Bantsimba-Malanda C; Hervatin F; Marchal-Somme J; Michel JB; Le Guludec D; Billiald P; Jandrot-Perrus M, Non-Invasive Molecular Imaging of Fibrosis Using a Collagen-Targeted Peptidomimetic of the Platelet Collagen Receptor Glycoprotein VI. PLOS ONE 2009, 4 (5), e5585. [PubMed: 19440310]

(9). Zheng L; Ding X; Liu K; Feng S; Tang B; Li Q; Huang D; Yang S, Molecular imaging of fibrosis using a novel collagen-binding peptide labelled with 99mTc on SPECT/CT. Amino Acids 2017, 49 (1), 89–101. [PubMed: 27633720]

(10). Desogere P; Tapias LF; Hariri LP; Rotile NJ; Rietz TA; Probst CK; Blasi F; Day H; Mino-Kenudson M; Weinreb P; Violette SM; Fuchs BC; Tager AM; Lanuti M; Caravan P, Type I collagen–targeted PET probe for pulmonary fibrosis detection and staging in preclinical models. Sci. Trans. Med 2017, 9 (384), eaaf4696.

(11). Désogère P; Tapias LF; Rietz TA; Rotile N; Blasi F; Day H; Elliott J; Fuchs BC; Lanuti M; Caravan P, Optimization of a Collagen-Targeted PET Probe for Molecular Imaging of Pulmonary Fibrosis. J. Nucl. Med 2017, 58 (12), 1991–1996. [PubMed: 28611243]

(12). Tanzer ML, Cross-Linking of Collagen. Science 1973, 180 (4086), 561–566. [PubMed: 4573393]

(13). Kagan HM; Li W, Lysyl oxidase: Properties, specificity, and biological roles inside and outside of the cell. J. Cell. Biochem 2003, 88 (4), 660–672. [PubMed: 12577300]

(14). Chen HH; Waghorn PA; Wei L; Tapias LF; Schu Hle DT; Rotile NJ; Jones CM; Looby RJ; Zhao G; Elliott JM; Probst CK; Mino-Kenudson M; Lauwers GY; Tager AM; Tanabe KK; Lanuti M; Fuchs BC; Caravan P, Molecular imaging of oxidized collagen quantifies pulmonary and hepatic fibrogenesis. JCI Insight 2017, 2 (11).

(15). Waghorn PA; Jones CM; Rotile NJ; Koerner SK; Ferreira DS; Chen HH; Probst CK; Tager AM; Caravan P, Molecular Magnetic Resonance Imaging of Lung Fibrogenesis with an Oxyamine-Based Probe. Angew. Chem. Int. Ed 2017, 56 (33), 9825–9828.

(16). Agarwal P; van der Weijden J; Sletten EM; Rabuka D; Bertozzi CR, A Pictet-Spengler ligation for protein chemical modification. Proc. Natl. Acad. Sci 2013, 110 (1), 46–51. [PubMed: 23237853]

(17). Wahsner J; Gale EM; Rodriguez-Rodriguez A; Caravan P, Chemistry of MRI Contrast Agents: Current Challenges and New Frontiers. Chem. Rev 2019, 119 (2), 957–1057. [PubMed: 30350585]

(18). Dirksen A; Dawson PE, Rapid Oxime and Hydrazone Ligations with Aromatic Aldehydes for Biomolecular Labeling. Bioconj. Chem 2008, 19 (12), 2543–2548.

(19). Kölmel DK; Kool ET, Oximes and Hydrazones in Bioconjugation: Mechanism and Catalysis. Chem. Rev 2017, 117 (15), 10358–10376. [PubMed: 28640998]

(20). Waghorn PA; Oliveira BL; Jones CM; Tager AM; Caravan P, High sensitivity HPLC method for determination of the allysine concentration in tissue by use of a naphthol derivative. J. Chromatogr. B Analyt. Technol. Biomed. Life Sci 2017, 1064, 7–13.

(21). Liu T; De Los Santos FG; Phan SH Fibrosis: Methods and Protocols, Rittié L, Ed. Springer New York: New York, NY, 2017; 27–42.

(22). Srivastava AK; Khare P; Nagar HK; Raghuwanshi N; Srivastava R, Hydroxyproline: A Potential Biochemical Marker and Its Role in the Pathogenesis of Different Diseases. Curr. Prot. Peptide Science 2016, 17 (6), 596–602.

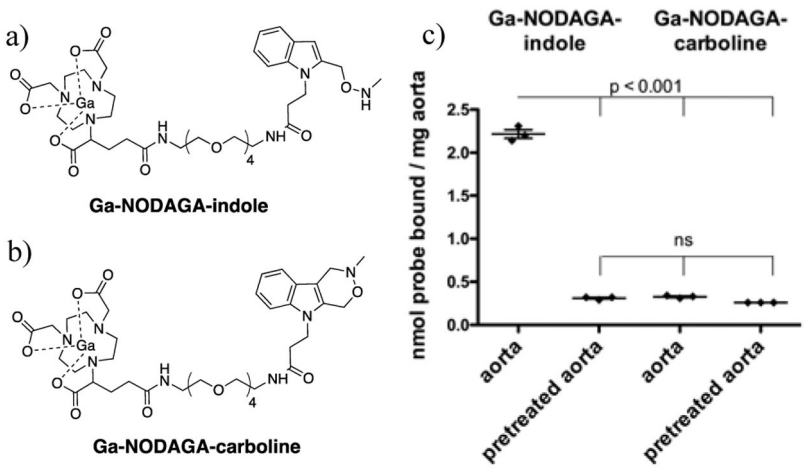

Figure 1.

(a) Allysine-reactive probe Ga-NODAGA-indole and (b) non-reactive analog Ga-NODAGA-carboline. (c) ^{nat}Ga-NODAGA-indole and ^{nat}Ga-NODAGA-carboline binding to porcine aorta or aorta pretreated with an excess of aldehyde reactive compound showing that ^{nat}Ga-NODAGA-indole binds specifically to allysine-rich tissue. n = 3 per experiment using different segments of porcine aorta from the same animal. Data were analyzed with one-way analysis of variance (ANOVA), followed by post-hoc Tukey tests.

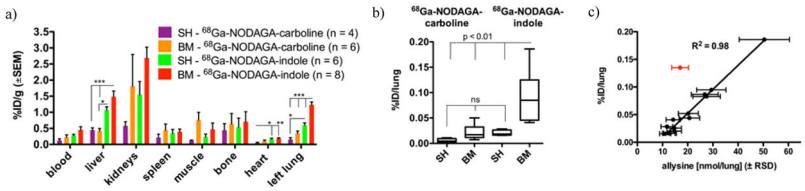

Figure 2.

(a) Ex vivo distribution of ^{68}Ga-NODAGA-indole and ^{68}Ga-NODAGA-carboline 2 h post injection, expressed as percent injected dose per gram of tissue (%ID/g) (mean ± SE) in various organs. (b) Ex-vivo uptake of ^{68}Ga-NODAGA-indole and ^{68}Ga-NODAGA-carboline in lungs from sham- (n=10) and bleomycin-treated (n=14) mice 2 h post injection, expressed as %ID/lung. The uptake of ^{68}Ga-NODAGA-indole in fibrotic lungs is 7-fold higher than in sham animals and 7- or 8-fold higher than the lung uptake of ^{68}Ga-NODAGA-carboline in bleomycin- or sham-treated mice, respectively. (c) Strong correlation (R^2=0.98, $p < 0.0001$) between lung uptake of ^{68}Ga-NODAGA-indole and allysine content in sham- (n=6) and bleomycin-treated (n=8) mice, (one outlier is highlighted in red, which was not included in the linear regression analysis). Data in 2a and 2b were analyzed with one-way ANOVA, followed by post-hoc Tukey tests; * $p < 0.05$, ** $p < 0.01$, *** $p < 0.001$.

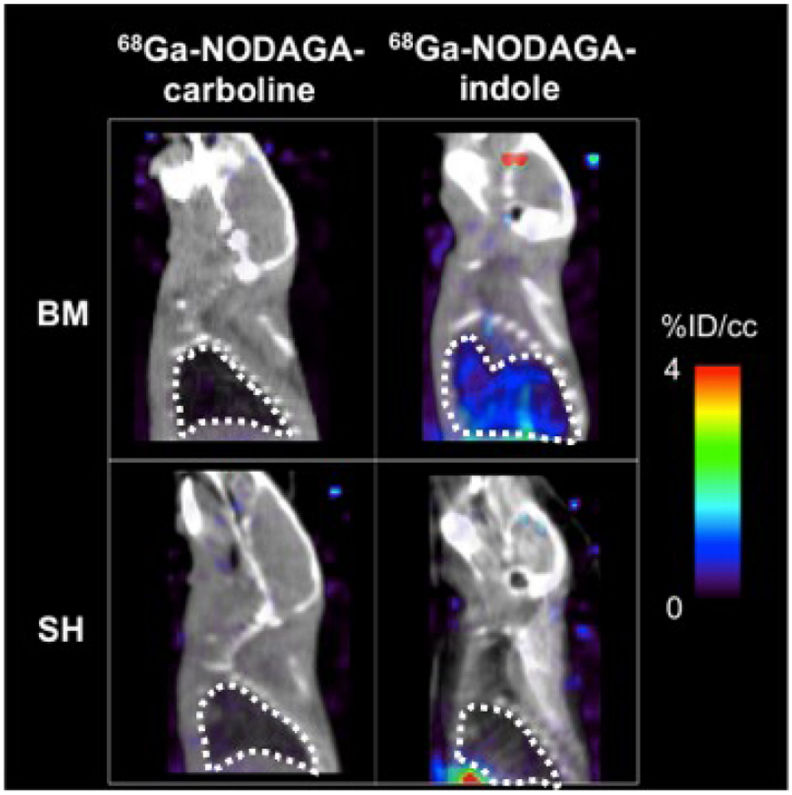

Figure 3.

Representative fused PET (color scale) – CT (greyscale) sagittal images of the head and thorax 110 – 120 min post injection of (left) ^{68}Ga-NODAGA-carboline and (right) ^{68}Ga-NODAGA-indole in sham- (SH, bottom) and bleomycin-treated (BM, top) animals; the lung is highlighted with a dashed white line. The PET signal, expressed as %ID/cc, in the lung is low in both sham and BM treated mice with ^{68}Ga-NODAGA-carboline, but is higher in the BM treated mouse imaged with ^{68}Ga-NODAGA-indole demonstrating the specificity of the latter probe for fibrogenesis.

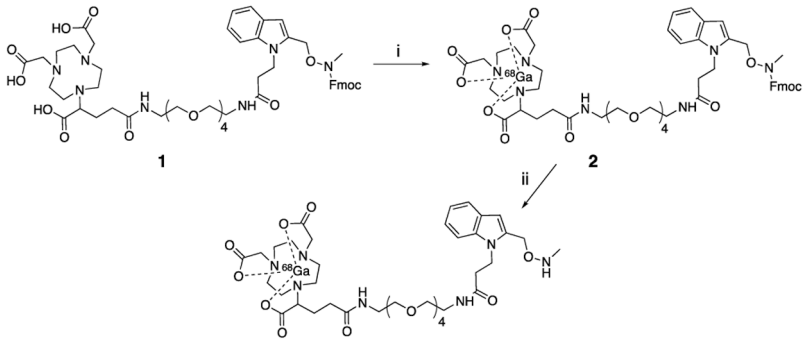

Scheme 1.
Preparation of ^{68}Ga-NODAGA-indole.[a]